

SEISMOLOGICAL EVIDENCE FOR A SUB-VOLCANIC ARC MANTLE WEDGE
BENEATH THE DENALI VOLCANIC GAP, ALASKA

Daniel E. McNamara

USGS, Golden, CO

Michael E. Pasyanos

Lawrence Livermore National Laboratory, Livermore, CA

manuscript in review: Geophysical Research Letters January 2002: PREPRINT

Correspondence to:

Daniel E. McNamara

USGS

1711 Illinois St.

Golden, CO 80401

(303) 273-8550 VOICE

(303) 273-8600 FAX

mcnamara@usgs.gov

Abstract. Arc volcanism in Alaska is strongly correlated with the 100km depth contour of the western Aluetian Wadati-Benioff zone. Above the eastern portion of the Wadati-Benioff zone however, there is a distinct lack of volcanism (the Denali volcanic gap). We observe high Poisson's ratio values (0.29-0.33) over the entire length of the Alaskan subduction zone mantle wedge based on regional variations of P_n and S_n velocities. High Poisson's ratios at this depth (40-70km), adjacent to the subducting slab, are attributed to melting of mantle-wedge peridotites, caused by fluids liberated from the subducting oceanic crust and sediments. Observations of high values of Poisson's ratio, beneath the Denali volcanic gap suggest that the mantle wedge contains melted material that is unable to reach the surface. We suggest that its inability to migrate through the overlying crust is due to increased compression in the crust at the northern apex of the curved Denali fault.

Introduction

The Alaska subduction zone formed as a result of the northward migration of the Pacific plate beneath the continental margin of North America along the Aleutian megathrust. This subduction zone is characterized by active seismicity, arc volcanism and mountain building. The Pacific plate drifts in a northwesterly direction (5-6 cm/yr), subducting at a relatively shallow angle (10-15°) until it bends and dives steeply (55°) beneath the volcanic arc (figure 1) [Ratchkovsky *et al.*, 1997]. The chain of strato volcanoes correlates strongly with the 100 km depth contour of the western Wadati-Benioff zone (WBZ), however volcanic activity ends abruptly with Spurr and Hayes, roughly 320 km west of the eastern termination of seismicity (Figure 1). This paucity of

volcanism has been termed the Denali volcanic gap [Nye, 1999] and has been attributed to: (1) extensive de-watering in the wide arc-trench gap due to the shallow subduction angle, causing the infertile slab to lack necessary fluids for arc magma generation; or (2) a thick continental crust under the Alaska range that inhibits the rise of arc magma.

To understand the subduction/volcanic process in Alaska we model the travel times of regional Pn and Sn phases, and solve for lateral seismic velocity variations in both the crust and upper mantle. Pn and Sn are regional distance head-waves that refract at the Moho and travel in the uppermost mantle. Pn and Sn velocities are most sensitive to temperature and composition in the upper mantle, which can be a strong indicator of tectonic environment. Estimates of Poisson's ratio, based on Pn and Sn velocities, are relatively insensitive to temperature, but provide better constraints on composition and partial melt content than P or S models alone.

Data and Method

We modeled the travel times of regional Pn and Sn body waves from 2246 crustal earthquakes recorded at 221 stations operated by the Alaska Volcano Observatory (AVO), Alaska Tsunami Warning Center (ATWC), Alaska Earthquake Information Center (AEIC) and Global Seismic Network (GSN) during the period September 1998 through September 2000 (Figure 2). AEIC hypocentral locations were used for events smaller than mb 5.0, while larger event locations were taken from the USGS Preliminary Determination of Epicenters earthquake catalog. To isolate regional phases (Pn , Sn), we selected travel times within a narrow distance range (200-1100 km). Between these distances the travel times are linear, suggesting an insignificant mantle velocity gradient. At regional distances of 200-1100 km, Pn and Sn should be head-waves, bottoming at depths no more than 20-30 km beneath the Moho [Hearn and Clayton, 1986].

To further ensure that only well recorded ($M_L \geq 3.0$) crustal events were included, hypocenter depths were restricted to < 20 km, and the refractor depth for the inversion was set to the continental crustal thickness (40 km) [Biswas and Tytgat, 1988]. Large travel time residuals are common across the seismic network due to systematic misidentification of phases, measurement errors and velocity model uncertainty. In order to minimize modeling uncertainties we used only first arrivals in the AEIC catalogs and required individual event/station apparent velocity perturbations to be within 15% of the

linear fit to the regional Pn data set ($Vp=8.2$ km/s). The same selection criteria were applied to the Sn dataset using an average $Vs=4.3$ km/s, which effectively eliminated commonly misidentified phases such as Lg . By applying these strict criteria to nearly 200,000 AEIC picks, the data set was culled to 54,036 high-quality Pn and 14,843 Sn travel times. Any remaining travel time residuals are attributed to lateral velocity variations within the upper mantle and crust. Figure 2 shows the resultant distribution of ray paths across the region.

We use a tomographic inversion procedure to solve for the lateral velocity structure. Standard regional phase tomographic studies [i.e. *Hearn and Clayton, 1986*] generally model lateral variations in the mantle using a single block layer and in the crust by computing static corrections for stations and events. The disadvantage of this technique is that the crustal statics are completely independent of one another. As a result, the crustal statics are often highly variable and difficult to interpret in terms of crustal velocity structure.

In this study we parameterize our model by using two layers of blocks, one for the upper mantle and a second for the crust. This technique has the advantage of forcing consistent crustal transits between adjacent earthquakes and stations. This method has been used to invert for compressional velocity in the crust and upper mantle along the Tethys collision zone [*Pasyanos et al., 2002*]. Details of the methodology are left to this paper. Using this method, we find that the crustal velocities vary smoothly across the model and are generally easier to interpret in terms of tectonic structure. In addition, we impose smoothness on our model by constraining the Laplacian of the slownesses in the crust and mantle to be zero. Weighting factors control the tradeoff between fitting the travel times and smoothing the model. We chose a 0.5 degree by 0.5 degree grid for the inversion. We solve the system of equations using the conjugate gradient method, a search technique that works well on sparse linear systems like the travel time problem.

Resolution. A qualitative measure of model resolution can be obtained by inspecting the ray path density and distribution within a particular region (Figure 2). Coverage is best throughout south-central Alaska (the Anchorage to Fairbanks corridor). Quantitative estimates of the model resolution were obtained by computing synthetic travel times for alternating-velocity "checkerboard" test models, given our source-

receiver distribution, and then inverted in the same manner as the observed data set. By comparing the inversion results to the input test models, the resolution of the data set can be assessed across the sampled region. Using a range of test models, we estimate a minimum anomaly size of about 3 degrees with 3% velocity perturbation is resolvable with the Pn data set. Model resolution is best in south-central Alaska, where raypath density and azimuthal distribution is greatest.

Results

The starting model is determined by the linear fit to the travel times, ($Pn=8.2\text{km/s}$, $Sn=4.3\text{km/s}$). We then solved for lateral velocity perturbations in the crust and upper mantle. The inversions ran for 15 iterations, after which both the variance reduction and model velocity perturbations stabilized. P -wave residuals were reduced from an initial RMS of 4.2 s to 1.8 s, a 58% variance reduction. S -wave residuals were reduced from 8.0 s to 1.4 s after 15 iterations for a variance reduction of 81%. Results of the inversion for the P -wave and S -wave velocities of the upper mantle are shown in Figure 3.

Since there is a strong tradeoff between crustal thickness and velocity, it is difficult to interpret the crustal models in detail. There could also be some contamination from large depth errors in event location, which could map biases into crustal velocities in regions with sparse coverage. However, we do find that the large general features in the crustal velocity models correlate well with major surface geological features. For example, prominent low P and S -wave velocity anomalies are associated with the thick sediments of the Cook Inlet and the intensely faulted and thickened crust of the Alaska Range. Also, average crustal Pg velocities from active source studies are consistent with our results in the Prince William Sound region [Brocher *et al.*, 1994].

Variations in Pn and Sn velocity can be directly related to thermal or compositional differences in the upper mantle resulting from different tectonic environments. The global average Pn velocity is 8.09 ± 0.20 km/s ($Sn=4.67$ km/s, assuming a Poisson's solid, $\sigma=0.25$) [Christensen and Mooney, 1995] and deviations in upper mantle velocities correlate well with the time since the last thermotectonic event. For example, continental shields and platforms have a higher Pn velocity (8.1-8.4 km/s) while continental orogens and rifts are lower (7.9-8.0 km/s).

The velocity structure of the upper mantle in Alaska is characterized by significant lateral variation ($P_n=7.85-8.45$ km/s, $S_n=4.05-4.65$ km/s) that correlates well with upper mantle structures expected in a subduction zone (Figure 3). For example, we observe relatively low P_n (7.85-8.0 km/s) and S_n (4.05-4.25 km/s) velocities in the uppermost mantle along the length of the volcanic arc, beneath the Alaska Range and the Wrangell Mountains (Figure 3). This is expected given the presence of fluids and relatively high temperatures within the sub-volcanic arc mantle wedge in an active subduction zone [Fuis and Plafker, 1991; Nolet and Zielhuis, 1994].

A second, striking observation is the prominent high seismic velocity ($P_n=8.25-8.45$ km/s, $S_n=4.4-4.66$ km/s), in the upper mantle along the southern coast of continental Alaska and the Aleutian island chain. This feature is interpreted as the Pacific slab penetrating the mantle at a depth interval of 40-70 km. We observe a P_n velocity amplitude variation of about 6-7% between the slab and the overriding mantle wedge ($S_n\sim 15\%$). Velocity amplitude variations of this magnitude are commonly observed in active subduction zones, including Alaska [Kissling and Lahr, 1991; Zhao *et al.*, 1995; Sadeghi *et al.*, 2000; Mele *et al.*, 1998].

In the Prince William Sound region we observe P_n velocities in the range of 8.0-8.1 km/s. Such velocities are consistent with previous active-source experiments in the region and have been interpreted as imbricated subduction of the Pacific Plate and Chugach terrane beneath continental Alaska [Brocher *et al.*, 1994].

Discussion and Conclusions

The general pattern of upper mantle velocity anomalies in our model can be described by: 1) low P_n and S_n velocities associated with the subcontinental upper mantle wedge; and 2) higher P_n and S_n velocities associated with the subducting Pacific plate. P_n and S_n velocities are most sensitive to upper mantle temperature and composition or a combination of these physical properties [McNamara *et al.*, 1997]. Determining the tectonic characteristics of the Alaskan subduction zone requires constraints on these physical properties and composition may be the most diagnostic tectonic indicator. The elastic parameter Poisson's ratio (σ), the ratio of radial contraction to axial elongation, can be computed using both P and S -wave velocity models, and provides compositional constraints not available with either P or S -wave velocity alone. Values for common rock

types range from $\sigma=0.20-0.35$. Laboratory derived values pertinent to our study include: average continental crust ($\sigma=0.26$); average oceanic crust ($\sigma=0.30$); serpentinized mantle peridotites ($\sigma>0.30$); and subducted oceanic lithosphere ($\sigma=0.25$) [Christensen, 1972; 1996]. Several seismic studies have demonstrated the effectiveness of estimating Poisson's ratio for determining the bulk composition of the crust and upper mantle [Zandt and Ammon, 1995; Rodgers and Schwartz 1998; Kamiya and Kobayashi, 2000]. For this reason we have combined our Pn and Sn models to produce a map of Poisson's ratio in the upper mantle beneath the Alaska subduction zone (Figure 4).

The resolution of our upper mantle Poisson's ratio is limited by the Sn model and is most reliable within the region shown in Figure 4. We observe low σ , on the order of 0.23-0.27, along the north side of the Aleutian megathrust, where the oceanic slab penetrates the upper mantle. This range of values is consistent with σ expected for subducting oceanic lithosphere [Christensen, 1996] and is supported by our observation of high Pn and Sn velocities in the same region (Figure 3). Beneath the eastern end of the volcanic arc, trending northeast into the Denali volcanic gap and well into the Alaska Range, we observe a range of very high values of Poisson's ratio ($\sigma=0.29-0.33$). Highs beneath the eastern Aleutian volcanic arc and Denali volcanic gap reach $\sigma=0.31-0.33$. Values this high are rare but have been observed in the mantle wedge beneath the Japanese subduction zone [Kamiya and Kobayashi, 2000]. In addition, Rodgers and Schwartz [1998] measured σ as high as 0.30 in the partially molten upper mantle beneath the Qiantang terrane of the northern Tibetan Plateau. Based on these previous studies two possible explanations exist for such high values of Poisson's ratio in the mantle wedge: (1) hydrated mantle wedge peridotites due to fluids liberated from the subducting slab; (2) partial melt of the sub-volcanic arc mantle wedge. We favor a combination of both, where hydrated peridotites induce melt in the wedge, for the following reasons. First, our observed low Pn and Sn velocities, and high Poisson's ratio are very consistent with hydrous serpentinized peridotite at 1 GPa [Christensen, 1972]. Second, thermal modeling of the Alaska subduction zone indicates that the mantle wedge adjacent to the slab lies at subsolidus conditions and is not partially molten. Partial melt however, does exist in the core of the wedge. Furthermore, numerous hydrous peridotite phases are stable under such subsolidus conditions and are present in the wedge [Ponko and Peacock, 1995].

Third, slab dehydration was employed to explain high b -value anomalies at a depth interval of 70-100 km beneath the Cook Inlet and the Alaska Range [Weimer and Benoit, 1996]. Finally, the trace element signature of magmas from eastern end stratovolcanoes and the Buzzard creek Maars document extensive modification of the subvolcanic mantle wedge by slab-transported fluids [Nye, 1999] (Figures 1 and 5). While we cannot resolve the individual contribution of each process with our study, both imply that the subarc mantle wedge is in a state capable of generating the magmas necessary to supply the surface volcanoes.

Denali volcanic gap. Our most significant observation is that the Alaska range, in the region of the Denali volcanic gap, is underlain by a mantle wedge similar in composition and thermal properties to the sub volcanic arc mantle, beneath the Cook Inlet. This observation leads to the question: Why are there no volcanoes in the Denali volcanic gap? Two possible reasons for a lack of volcanism in this region have previously been proposed [Nye, 1999]: (1) extensive de-watering in the wide arc-trench gap, causing the infertile slab to lack necessary fluids for arc magma generation; (2) a thick continental crust under the Alaska range that inhibits the rise of arc magma. New evidence of the existence of the 3000 year old Buzzard Creek arc-basalt magmas, directly above the eastern edge of the slab (Figures 1 and 4), do not support (1) and argue that the Pacific plate is able to transport fluids necessary for magma generation, 500 km into continental Alaska. In addition, recent and active volcanism associated with thick continental crust in the Altiplano of Bolivia and the Tibetan plateau (70-80 km) would argue against (2), since the crust of the Alaska range likely never exceeds 40 km. We propose an alternate solution in which increased stress on the concave side of the curved Denali fault system (DFS) inhibits the rise of magma through a crust under compression. The increased compression is a result of a space problem at the northern apex of the curved fault system.

The DFS is a ~1200 km strike-slip fault system, extending from southeast Alaska and arcing well into central Alaska (Figure 1), along which the crust is actively deforming at a rate of 1-2 cm/yr [Plafker *et al.*, 1977; Fletcher and Freymueller, 1998]. The DFS is generally regarded as a right-lateral strike-slip fault, with 200-400 km offsets along the central and eastern limbs [Stout and Chase, 1980]. Offsets on the western end of the DFS

are poorly constrained and considerably more contentious. For example *Csejtey et al.*, [1982] suggest that the western limb of the DFS has been locked throughout the Tertiary, while *Redfield and Fitzgerald* [1993] argue that the western DFS has undergone significant left-lateral motion.

Schultz and Aydin [1990] modeled displacements and stresses along the curved DFS in a regional stress state inferred from Tertiary relative plate motion directions. They found that mean stress due to late Tertiary slip is increased by 10% above background levels of the surrounding region on the concave side of the bend and reduced by 10% on the convex side. The overall stress pattern agrees well with both regional topography and crustal earthquake focal mechanisms. For example, the lowlands of the Tanana basin are located north of the DFS, on the convex low-stress side, while Alaska Range uplift is found to the south on the concave, high stress, side of the DFS (Denali massif, figure 1). Also, reverse fault mechanisms have been computed for crustal events south of the DFS (Figure 4) [*Ratchkovsky and Hansen*, 2002]. Despite the disagreement in Tertiary displacements along the DFS it is clear that its curved shape creates a space problem at its northern apex, causing increased crustal compression, on the concave side, relative to surrounding regions. *Fitzgerald et al.*, [1993] suggest that the Denali massif was rapidly uplifted ~5-6 Ma as a direct result of increased stress on the concave side of the DFS, due to a change in the direction of Pacific plate motion [*Cox and Engebretson*, 1985].

In conclusion, we suggest that the increased crustal compression in the Denali region, on the concave side of the bend in the DFS, would close potential conduits in the crust preventing magmas from migrating to the surface. The lack of volcanism in the Denali volcanic gap corresponds to uplift of the Denali massif due to an increase in compressional stress in the crust at the northern apex of the curved DFS.

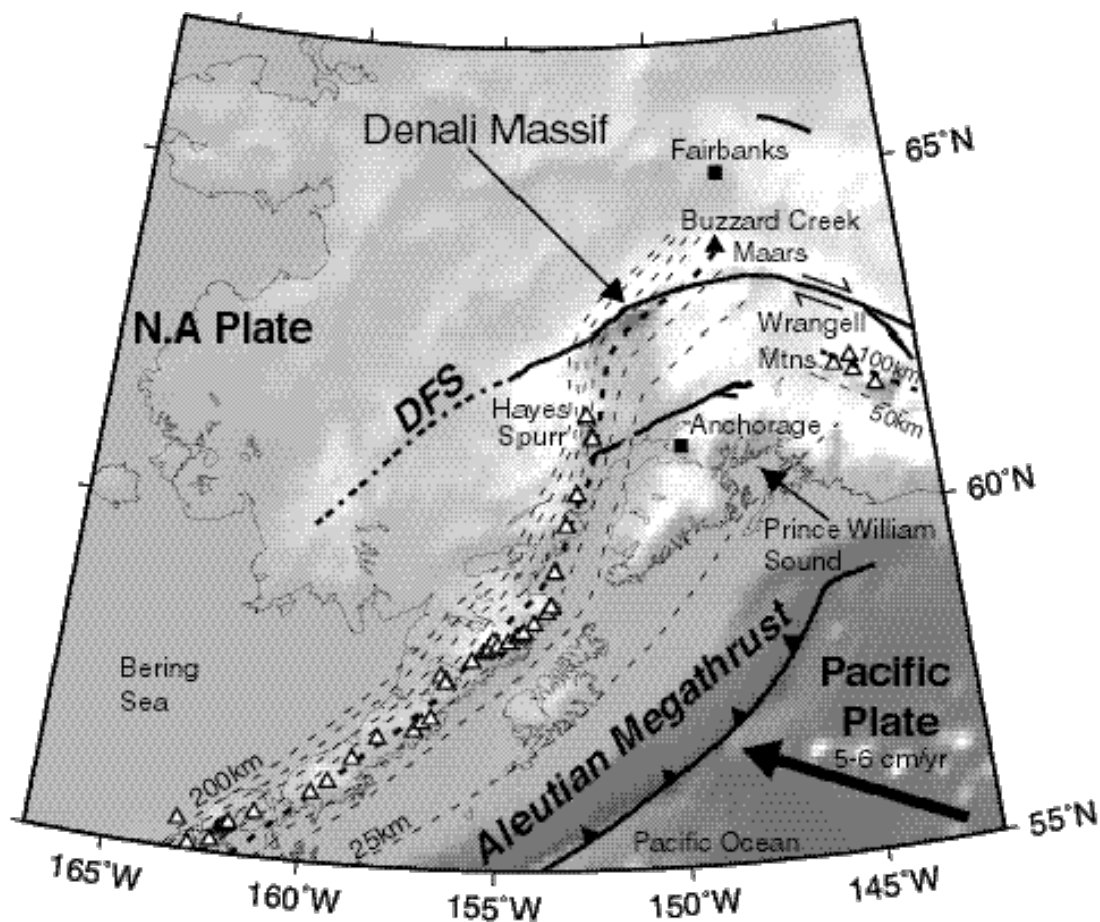
Acknowledgements. This paper benefited from comments by S. Fowell, H. Benz and J. Lahr. D.M expresses gratitude to AEIC, analysts: L. Rao, E. Clark, and M. LaFevers, who located the hypocenters used in this study. We thank the AEIC for use of their network phase data. Maps were creating using the GMT software [Wessel and Smith, 1991]. This work was performed under the auspices of the U.S. Department of Energy at the Lawrence Livermore National Laboratory under contract W-7405-ENG-48. This is LLNL contribution UCRL-JC-143289.

References

- Biswas, N., and G. Tytgat, Intraplate seismicity of western Alaska, *Seismo. Res. Lett.*, 59, 227-233, 1988.
- Brocher, T. M., G. S. Fuis, M. A. Fischer, G. Plafker, M. J. Moses, J. J. Tabor, and N. I. Christensen, Mapping the megathrust beneath the northern Gulf of Alaska using wide-angle seismic data, *J. Geophys. Res.*, 99, 11,663-11,685, 1994.
- Christensen, N. I., The abundance of serpentinites in the oceanic crust, *J. geol.*, 80, 709-719, 1972.
- Christensen, N. I., Poisson's ratio and crustal seismology, *J. Geophys. Res.*, 101, 3139-3156, 1996.
- Christensen, N. I., and W. D. Mooney, Sismic velocity structure and composition of the continental crust: a global view, *J. Geophys. Res.*, 100, 9761-9788, 1995.
- Cox, A., and D. D. C. Engebretson, Change in motion of Pacific plate at 5 m.y. B.P., *Nature*, 313, 472-474, 1985.
- Csejtey, B., D. P. Cox, R. C. Evarts, G. D. Stricker, and H. L. Foster, the Cenozoic Denali fault system and the Cretaceous development of southern Alaska, *J. Geophys. Res.*, 87, 3741-3752, 1982.
- Fitzgerald, P. F., E. Stump, and T. Redfield, Late Cenozoic uplift of Denali and its relation to relative plate motion and fault morphology, *Science*, 259, 497-489, 1993.
- Fletcher, H. J., and J. T. Freymueller, A GPS Study of Interior Alaska Deformation, *EOS, Trans. AGU*, 79 (45, suppl), 1998.
- Fuis, G. S., E. L. Ambos, W. D. Mooney, N. I. Christensen, and E. Geist, Crustal structure of accreted terranes in southern Alaska, Chugach Mountains and Coper River Basin, from seismic refraction results, *J. Geophys. Res.*, 96, 4187-4227, 1991.

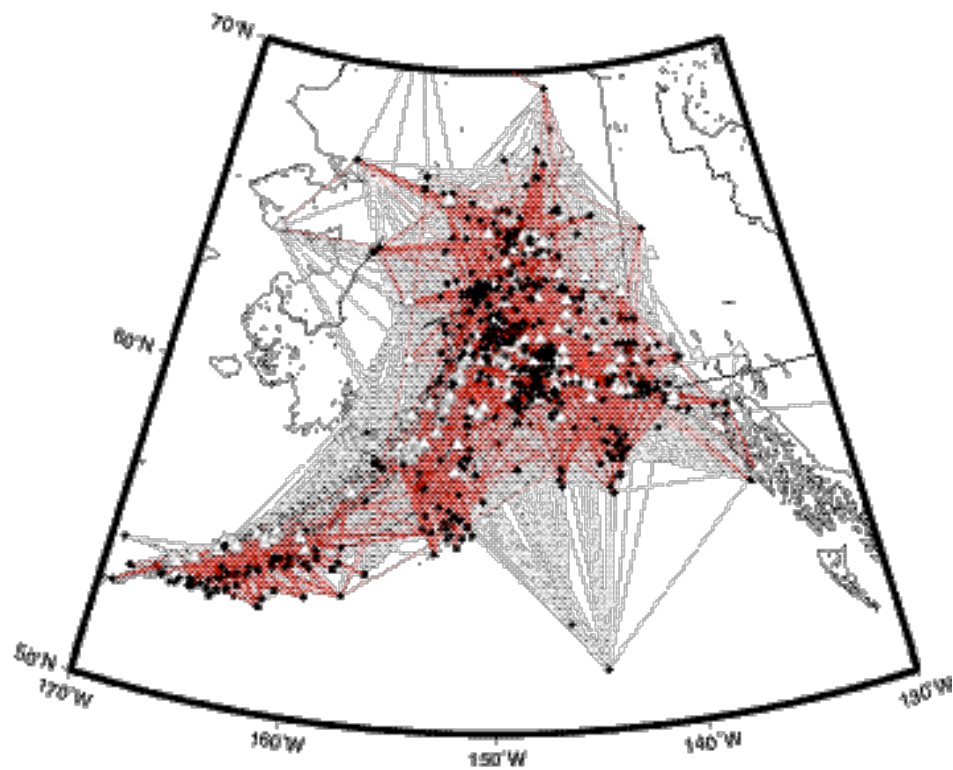
- Hearn, T.M. and R.W. Clayton, Lateral velocity variations in Southern California II. Results for the lower crust from Pn waves, *Bull. Seism. Soc. Am.*, 76, 511-520, 1986.
- Kamiya, S., and Y.Kobayashi, Seismological evidence for the existence of serpentinized mantle wedge, *Geophys. Res Lett.*, 27, 819-822, 2000.
- Kissling, E. and J. Lahr, Tomographic image of the Pacific slab under southern Alaska, *Ecolgae Geol. Helv.*, 84, 297-315, 1991.
- McNamara, D.E., W.R. Walter, T.J. Owens, and C.J. Ammon, Upper mantle velocity structure beneath the Tibetan plateau from Pn travel time tomography, *J. Geophys. Res.*, 102, 493-505, 1997.
- Mele, G., A. Rovelli, D. Seber, T. Hearn, and M. Barazangi, Compressional velocity structure and anisotropy in the uppermost mantle beneath Italy and surrounding regions, *J. Geophys. Res.*, 103, 12,529-12,543, 1998.
- Nolet, G. and A. Zielhuis, Low S velocities under the Tornquist-Teisseyre zone: Evidence for water injection into the transition zone by subduction, *J. Geophys. Res.*, 99, 15813-15820, 1994.
- Nye, C., The Denali Volcanic Gap-Magmatism at the Eastern End of the Aleutian Arc. *Eos*, 80, (46 suppl.), p. 1203, 1999.
- Page, R. A., C. D. Stephens, and J. C. Lahr, Seismicity of the Wrangell and Aleutian Wadati-Benioff zones and the North American plate along the Trans-Alaska crustal transect, Chugach Mountains and Copper river Basin, southern Alaska,
- Pasyanos M. E., C.A. Schultz, W. R. Walter, W. G. Hanley, and D. E. McNamara, Compressional Velocity of the Uppermost Mantle Along the Tethys Collision Zone, *in prep*, 2002.
- Plafker, G., T. Hudson, and D. H. Richter, Preliminary observations on late Cenozoic displacements along the Totschunda and Denali fault systems, *U.S. Geol. Surv. Circ.*, 751-B, B67-B69, 1977.
- Ponko, S. C., and S. M. Peacock, Thermal modeling of the southern Alaska subduction zone: Insight into the petrology of the subducting slab and overlying mantle wedge, *J. Geophys. Res.*, 100, 22,117-22,128, 1995.

- Ratchkovsky, N. A., and R. Hansen, New constraints on tectonics of Interior Alaska: Earthquake locations, source mechanisms and stress regime, *Bull. Seism. Soc. Am.*, 92, 998-1014, 2002.
- Ratchkovsky, N. A., J. Pujol, and N. Biswas, Relocation of events in the Cook Inlet area, south central Alaska using the Joint Hypocenter Determination method, *Bull. Seism. Soc. Am.*, 87, 620-636, 1997.
- Redfield, T. F., and P. G. Fitzgerald, Denali fault system of southern Alaska: an interior strike-slip structure responding to dextral and sinistral shear coupling, *Tectonics*, 12, 1195-1208, 1993.
- Rodgers, A., and S. Y. Schwartz, Lithospheric structure of the Qiantang terrane, northern Tibetan Plateau, from complete regional waveform modeling: evidence for partial melt, *J. Geophys. Res.*, 103, 7137-7152, 1998.
- Sadeghi, H., S. Suzuki and H. Takenaka, tomographic low-velocity anomalies in the uppermost mantle around the northeastern edge of Okinawa trough, the backarc of Kyushu, *Geophys. Res. Lett.*, 27, 277-280, 2000.
- Schultz, R., and A. Aydin, Formation of interior basins associated with curved faults in Alaska, *Tectonics*, 9, 1387-1407, 1990.
- Stout, J. H., and C. G. Chase, Plate kinematics of the Denali fault system, *Can. J. Earth Sci.*, 17, 1527-1537, 1980.
- Weimer, S., and J. P. Benoit, Mapping the b-value anomaly at 100 km depth in the Alaska and New Zealand subduction zones, *Geophys. Res. Lett.*, 23, 1557-1560, 1996.
- Wessel, P. and W. Smith, Free software helps display data, *EOS*, 72, 445-446, 1991.
- Zandt, G., and C. J. Ammon, Continental crust composition constrained by measurements of crustal Poisson's ratio, *Nature*, 374, 152-154, 1995.
- Zhao, D., D. Christensen, and H. Pulpan, Tomographic imaging of the Alaska subduction zone, *J. Geophys. Res.*, 100, 6487-6504, 1995.



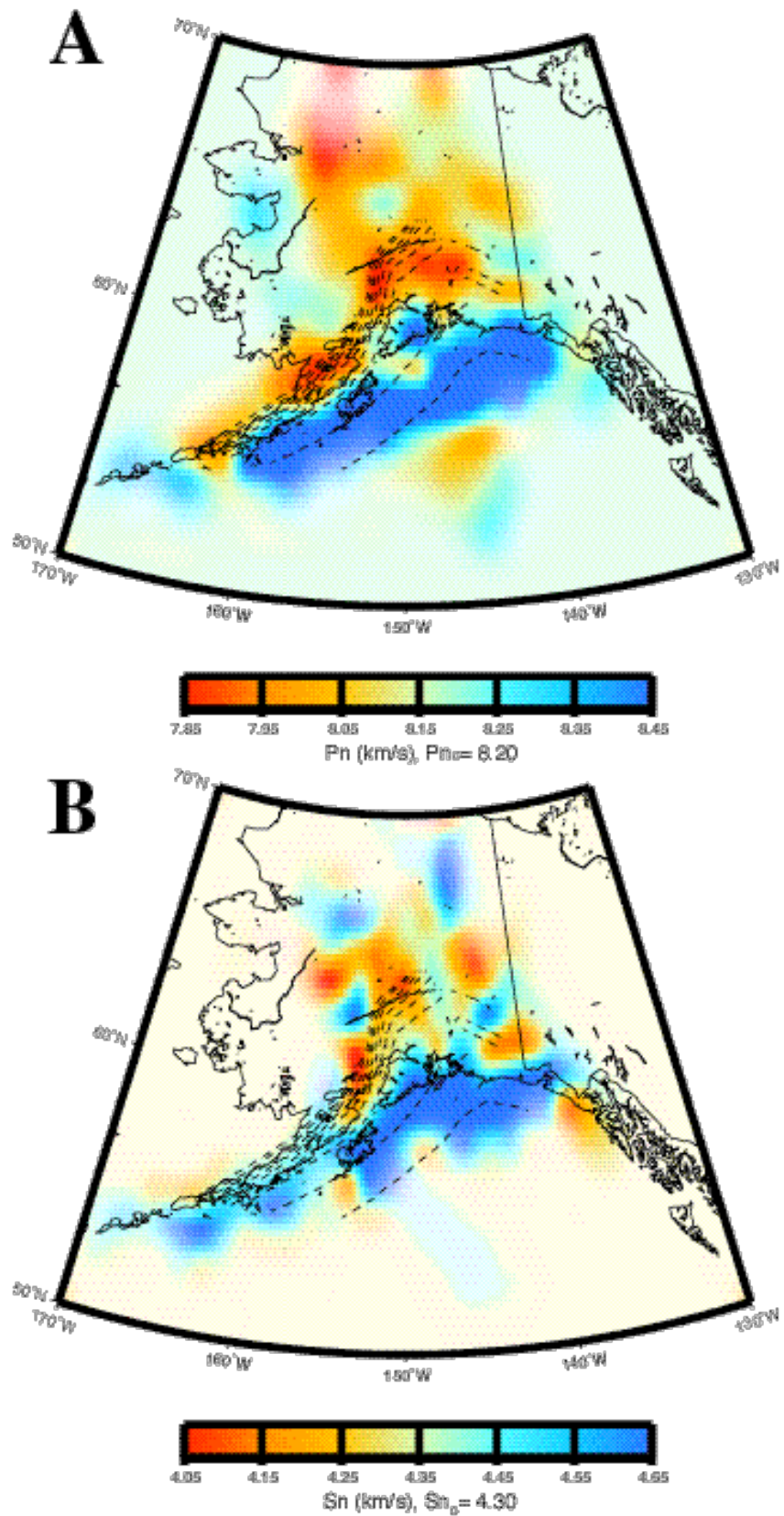
(Figure 1: McNamara and Pasyanos, 2002)

Figure 1: Alaska tectonic base map showing active volcanoes (white triangles) [Nye, 1999]; faults (solid black lines); Denali fault System (DFS); Pacific slab depth contours from 25-200 km, in 25 km intervals (dashed lines) 100 km contour in bold dashed line [Ratchkovsky *et al.*, 1997; 1998] and Wrangell slab contours [Page *et al.*, 1989]. The Alaska Range is the high elevation region (white) bounded by the Denali fault system (DFS).



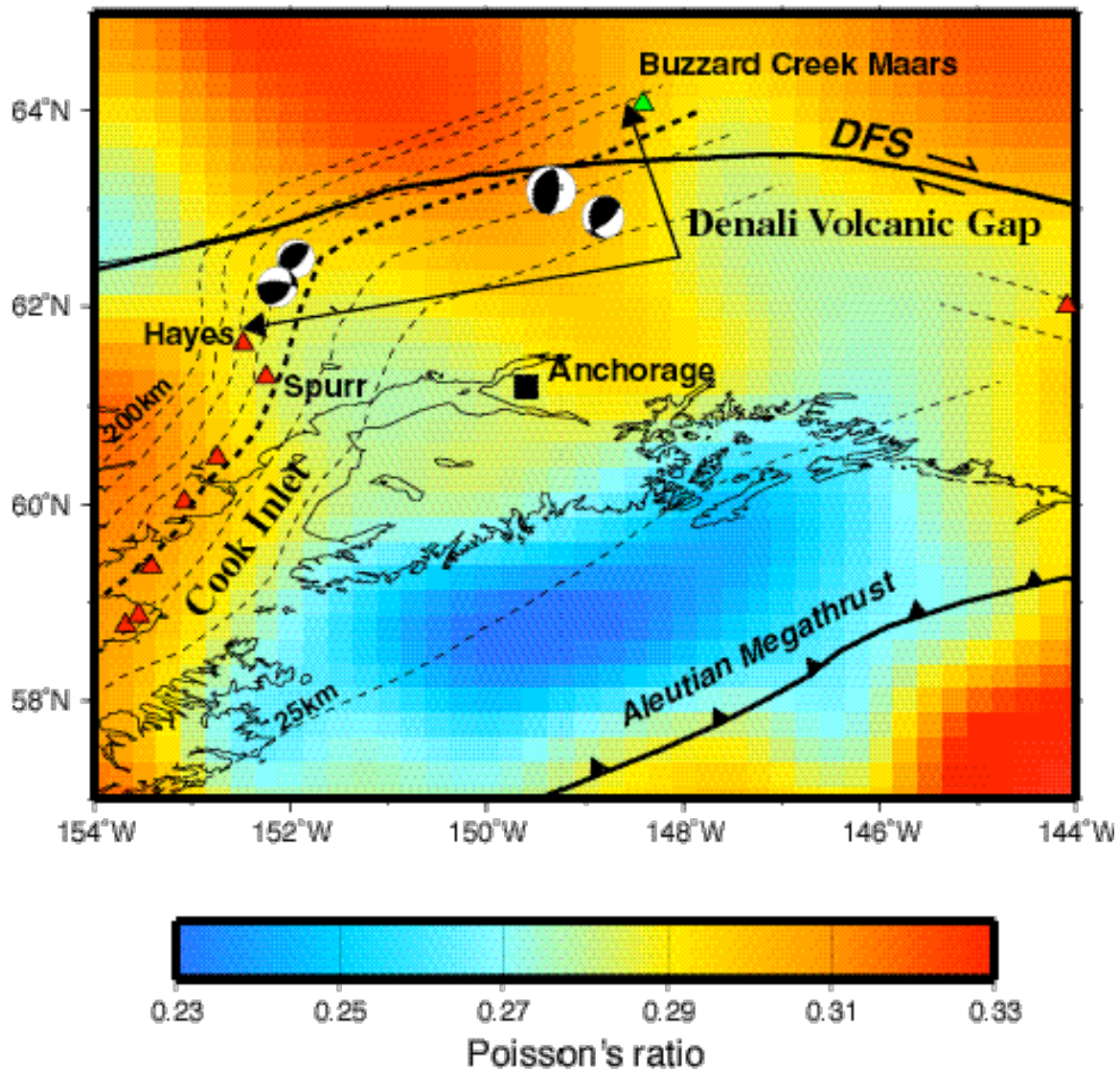
(Figure 2; McNamara and Pasyanos, 2002)

Figure 2: Alaska Pn , Sn path map showing 2246 earthquakes (black circles) and 221 recording stations (white triangles). (A) 54,036 Pn raypaths. (B) 14,843 Sn raypaths.



(Figure 4: McNamara and Pasyanos, 2002)

Figure 3: Mantle velocity models derived from Pn and Sn tomography. Pacific slab depth contours from *Ratchkovsky et al.*, [1997; 1998] and Wrangell slab contours from *Page et al.*, [1989]. (A) P -wave mantle model. (B) S -wave mantle model.



(Figure 4: McNamara and Pasyanos, 2002)

Figure 4: Poisson's ratio map of the uppermost mantle produced by combining the inversion results shown in Figure 4a and Figure 4b. The Denali volcanic gap is shown as the region between the easternmost volcano, Mt Hayes and the Buzzard Creeks Maars. Tectonic features include active volcanoes (red triangles) [Nye, 1999]; faults (solid black lines); Denali fault system (DFS); Pacific slab depth contours from 25-200 km, in 25 km intervals (dashed lines) 100 km contour in bold dashed line [Ratchkovsky *et al.*, 1997; 1998], Wrangell slab contours [Page *et al.*, 1989]., and reverse fault crustal focal mechanisms [Ratchkovsky and Hansen, 2002].